



Since January 2020 Elsevier has created a COVID-19 resource centre with free information in English and Mandarin on the novel coronavirus COVID-19. The COVID-19 resource centre is hosted on Elsevier Connect, the company's public news and information website.

Elsevier hereby grants permission to make all its COVID-19-related research that is available on the COVID-19 resource centre - including this research content - immediately available in PubMed Central and other publicly funded repositories, such as the WHO COVID database with rights for unrestricted research re-use and analyses in any form or by any means with acknowledgement of the original source. These permissions are granted for free by Elsevier for as long as the COVID-19 resource centre remains active.



Original article

Modulation of cell proteome by 25-hydroxycholesterol and 27-hydroxycholesterol: A link between cholesterol metabolism and antiviral defense

Andrea Civra^{a,1}, Mara Colzani^{b,1}, Valeria Cagno^c, Rachele Francese^a, Valerio Leoni^d, Giancarlo Aldini^b, David Lembo^a, Giuseppe Poli^{a,*}

^a Department of Clinical and Biological Sciences, University of Torino at San Luigi Hospital, Orbassano, Torino, Italy

^b Department of Pharmaceutical Sciences, Università degli Studi di Milano, Milan, Italy

^c Department of Molecular Microbiology, University of Geneva, Geneva, Switzerland

^d Department of Laboratory Medicine, University of Milano-Bicocca, School of Medicine, Hospital of Desio, Milano, Italy

ARTICLE INFO

Keywords:

Oxysterols
SILAC proteomics
25-Hydroxycholesterol
27-Hydroxycholesterol
Antiviral activity
Sterol metabolism

ABSTRACT

Physiological cholesterol metabolism implies the generation of a series of oxidized derivatives, whose oxysterols are by far the most investigated ones for their potential multifaceted involvement in human pathophysiology. In this regard, noteworthy is the broad antiviral activity displayed by defined side chain oxysterols, in particular 25-hydroxycholesterol (25HC) and 27-hydroxycholesterol (27HC). Although their antiviral mechanism(s) may vary depending on virus/host interaction, these oxysterols share the common feature to hamper viral replication by interacting with cellular proteins. Here reported is the first analysis of the modulation of a cell proteome by these two oxysterols, that, besides yielding additional clues about their potential involvement in the regulation of sterol metabolism, provides novel insights about the mechanism underlying the inhibition of virus entry and trafficking within infected cells. We show here that both 25HC and 27HC can down-regulate the junction adhesion molecule-A (JAM-A) and the cation independent isoform of mannose-6-phosphate receptor (MPRCi), two crucial molecules for the replication of all those viruses that exploit adhesion molecules and the endosomal pathway to enter and diffuse within target cells.

1. Introduction

Over the last few years solid evidence has been provided of a remarkable antiviral effect of defined oxysterols, essentially of enzymatic origin [1–3]. These cholesterol derived molecules proved to be effective in inhibiting the replication of a wide span of viral pathogens, characterised by highly divergent replicative strategies and structural features. In this relation, the most studied member of this family has certainly been 25-hydroxycholesterol (25HC), a physiological oxysterol whose production by the enzyme 25-cholesterol hydroxylase was proven to be interferon-inducible [1,2]. Moreover, a similarly strong inhibition of the replication of both enveloped and non-enveloped viruses was demonstrated to be exerted as well by 27-hydroxycholesterol (27HC) [4–6], the product of the ubiquitous

mitochondrial enzyme 27-cholesterol hydroxylase [7] and by far the most represented oxysterol in human plasma [8]. This unprecedented antiviral spectrum relies at least in part on the ability of oxysterols to modify the composition of cellular and subcellular membranes that all viral pathogens have to cross in order to enter the host cells or hijack their replicative machinery. These oxysterol-induced modifications can be triggered by different mechanisms such as (A) the direct interaction of oxysterols with cellular membranes, (B) the interaction with cellular proteins involved in cholesterol shuttling between intracellular membranes [such as the oxysterol-binding protein 1 (OSBP)], (C) the modulation of the expression of enzymes involved in cholesterol metabolism, by binding specific nuclear receptors such as the liver X receptor [LXR] and the estrogen receptor α [ER α] [3], or, last but not least, (D) a suitable potentiation of the initial inflammatory reaction by

* Corresponding author. at: Department of Clinical and Biological Sciences, University of Torino, San Luigi Hospital, RegioneGonzole 10, 10043 Orbassano, Torino, Italy.

E-mail addresses: andrea.civra@unito.it (A. Civra), mara.colzani@gmail.com (M. Colzani), valeria.cagno@unige.ch (V. Cagno), rachele.francese@unito.it (R. Francese), valerioleoni@hotmail.com (V. Leoni), giancarlo.aldini@unimi.it (G. Aldini), david.lembo@unito.it (D. Lembo), giuseppe.poli@unito.it (G. Poli).

¹ Authors equally contributed to the study.

<https://doi.org/10.1016/j.freeradbiomed.2019.08.031>

Received 30 June 2019; Received in revised form 19 August 2019; Accepted 30 August 2019

Available online 13 September 2019

0891-5849/ © 2019 Elsevier Inc. All rights reserved.

Abbreviations:

25HC	25-hydroxycholesterol	FBS	fetal bovine serum
27HC	27-hydroxycholesterol	DDA	data dependent acquisition
NFKB2	NF-kappa-B p100 subunit	CID	collision induced dissociation
LC	liquid chromatography	AUG	automatic gain control
MS	mass spectrometry	FDR	peptide false discovery rates
SILAC	stable isotope labelling by amino acids in cell culture	SDS-12% PAGE	sodium dodecyl sulphate-12% polyacrylamide gel electrophoresis
IFITM3	interferon-induced transmembrane protein 3	PVDF	polyvinylidene difluoride
MPRci	cation independent mannose-6-phosphate receptor	PBS	phosphate buffered saline
JAM-A	junctional adhesion molecule A	EDTA	ethylenediaminetetraacetic acid
LE	late endosomes	OSBP1	oxysterol binding protein 1
DMEM	Dulbecco's modified Eagle's medium	LXR	liver X receptor
		ER α	estrogen receptor α

cells under viral attack, for instance through a redox-dependent up-regulation of NF- κ B-driven overproduction of pro-inflammatory cytokines, in particular IL-6 [4].

Aiming at investigating the mechanism(s) behind such an important property of these side chain oxysterols, we deemed useful to afford the analysis of their possible modulation of cell proteome. To date, just two reports investigated the effect of not enzymatic 7-oxysterols on vascular cells proteome [9,10], while no data are so far accessible as far as side-chain and at the same enzymatic oxysterols are concerned.

2. Materials and Methods

2.1. Antibodies and reagents

The mouse monoclonal antibody directed to JAM-A (J10.4: sc-53623) was purchased from Santa Cruz Biotechnology, Inc. (Dallas, TX, USA). The mouse monoclonal antibody directed to actin (MAB1501R) was purchased from Millipore. The secondary antibody anti-mouse IgG horseradish (HRP)-linked (NA931V) was purchased from GE Healthcare UK (Chalfont St Giles, UK). 25HC and 27HC (Sigma) were dissolved in sterile ethanol at 3 mM.

2.2. Cell culture and SILAC labelling

Human epithelial adenocarcinoma HeLa cells (ATCC[®] CCL-2[™]) and African green monkey kidney epithelial cells (MA104) were propagated in Dulbecco's modified Eagle's medium (DMEM) (Gibco-BRL, Gaithersburg, MD) supplemented with heat-inactivated 10% fetal bovine serum (FBS) (Gibco/BRL) and 1% penicillin-streptomycin solution 100X (EuroClone), at 37 °C in an atmosphere of 5% of CO₂. HeLa cells were SILAC-labelled using SILAC DMEM (#89985, ThermoScientific) deficient in lysine and arginine, supplemented with 10% dialyzed fetal bovine serum (Invitrogen). To this medium, the appropriate amino acids were added as follows: unlabelled L-lysine (Lys0) and L-arginine (Arg0) (both from Sigma) were used to obtain light-labelled cells, and ¹³C₆¹⁵N₄ L-arginine (Arg10, CNLM-539, Cambridge Isotope Laboratory) and ¹³C₆¹⁵N₂ L-lysine (Lys8, CNLM-291, Cambridge Isotope Laboratory) were used to obtain heavy-labelled cells. The final amino acid concentration corresponded to the standard DMEM composition (i.e. 84 mg/l arginine and 146 mg/l lysine). Cells were cultured for at least seven replications to achieve complete labelling. Full protein labelling was verified by gelC-MS analysis (data not shown) [11].

2.3. Oxysterol treatment and preparation of cell extracts

Exponentially growing HeLa cells (either unlabelled or SILAC-labelled) were seeded in 10 cm dishes. After 24 h, cells were treated for 20 h with 25HC or 27HC at 5 μ M in SILAC DMEM supplemented with 2% dialyzed FBS. Control samples were prepared by treating cells with culture medium supplemented with equal volumes of ethanol,

corresponding to 0.17% (v/v) in cell media. For each oxysterol, a “direct” and a “reverse” protocol were performed according to the following scheme: for the “direct” experiment unlabelled HeLa cells were chosen as untreated control, while labelled HeLa cells were oxysterol-treated; for the “reverse” experiment, unlabelled HeLa were oxysterol-treated, while labelled HeLa were chosen as untreated control. After 20 h from treatment, cells were washed twice with phosphate buffered saline containing ethylenediaminetetraacetic acid (PBS/EDTA), trypsinized, washed with PBS and counted.

2.4. Protein extraction and digestion

Heavy-labelled and light-unlabelled HeLa cells were mixed in 1:1 proportion (5 million:5 million) to form direct and reverse SILAC samples, i.e. the four samples “direct 25HC”, “reverse 25HC”, “direct 27HC” and “reverse 27HC”. The mixed cells were pelleted and solubilized in Laemmli sample buffer (Bio-Rad) and dithiothreitol 50 mM, to extract proteins. The protein extract was centrifuged to pellet cellular debris (10 min, 16,000 g, 4 °C); 50 μ g of the clarified protein extracts were loaded on sodium dodecyl sulphate (SDS) polyacrylamide gel (any kD Mini Protean TGX, Bio-Rad). After protein electrophoresis (200 V for 25 min), the gel was stained with Coomassie blue (Bio-Safe, Bio-Rad). Each lane, corresponding to one SILAC sample, was cut into 14 subsequent bands of different molecular weight, in order to obtain a rough fractionation of the sample. Each gel slice was reduced with 10 mM dithiothreitol (Sigma) in 50 mM ammonium bicarbonate (Sigma) for 30 min at 56 °C and alkylated on cysteine residues by incubation with 55 mM iodoacetamide (Sigma) in 50 mM ammonium bicarbonate for 45 min at RT in the dark. Proteins were in-gel digested overnight using 1 μ g of trypsin (sequencing grade, Roche) solubilized in 50 mM ammonium bicarbonate, for each gel slice. Peptides were extracted from gel firstly with 30% acetonitrile/0.3% formic acid and then with 100% acetonitrile; the two extractions of each gel slice were pooled. Eluted peptides were dried in a vacuum concentrator (Martin Christ) and solubilized in 12 μ l of 0.1% formic acid.

2.5. Mass spectrometry analysis

Five μ l peptides solubilized in 0.1% formic acid were loaded on a nano C18 column (PicoFrit C18 HALO, 90 \AA , 75 μ m ID, 2.7 μ m, New Objective) by an RSLCnano System Ultimate 3000 (Dionex) controlled by the software Chromeleon Xpress (Dionex, version 6.80). Peptides were separated using a 90 min linear gradient (from 1% acetonitrile, 0.1% formic acid to 40% acetonitrile, 0.1% formic acid) and on-line electrosprayed into an LTQ Orbitrap XL mass spectrometer equipped with a nanospray ion source (both Thermo). The mass spectrometer operated in data dependent acquisition (DDA) mode, controlled by the software Xcalibur (version 2.0.7, Thermo) to acquire both full MS spectra in the m/z range 320–1400 (resolution 1×10^5 FWHM at m/z 400) and MS/MS spectra obtained by collision induced dissociation

(CID) of the 6 most abundant multi-charged ions. Automatic gain control (AUG) was set at 1×10^6 for the acquisition of full MS spectra and at 1×10^5 for MS/MS spectra. To avoid redundancy, after two subsequent occurrences in less than 30 s, precursor ions already selected for fragmentation were dynamically excluded for 45 s.

2.6. Protein identification and quantification

The software MaxQuant [12] (version 1.5.1.2) was used to extract peaks from spectra and to match them against the human protein database (downloaded on December 03.12.2014 from UniProt, 66922 entries). Mass values were re-calibrated using the “first search” option. The following main search was performed using the following parameters: enzyme = trypsin, maximum number of missed cleavages = 2, MS mass tolerance = 5 ppm, MS/MS mass tolerance = 0.3 Da, variable modification = oxidation of Met, fixed modification = carbamidomethylation of Cys. Spectra collected from the 14 fractions of the 4 SILAC samples were analysed simultaneously, by specifying the correct experimental design of the direct and reverse assays. The “re-quantify” and “match between runs” options were selected. The decoy mode based on the reverse database was activated; peptide false discovery rates (FDR) was set to 0.05 and protein FDR was set to 0.01.

2.7. Analysis of SILAC data

The four SILAC samples, namely “direct 25HC”, “reverse 25HC”, “direct 27HC” and “reverse 27HC” were analysed simultaneously to increase the number of protein identification and quantification. Then, the 25HC- and 27HC-treated samples were analysed separately, by considering the reverse and direct assay as independent replicate analyses. Rigorous quality filters were used to filter the “raw” protein list obtained by MaxQuant; only proteins identified by two peptides and at least by 1 unique peptide (in both replicates) were considered as genuine identifications and analysed further. Then only proteins quantified by at least two peptides (in both replicates) were analysed further.

For each replicate, the distribution of protein ratio was used to detect proteins up- and down-regulated by oxysterols, using as threshold the 5th and 95th percentile of the ratio distribution. Proteins with heavy/light (H/L) ratio > 95th percentile in the direct assay and < 5th percentile in the reverse assay were considered as up-regulated by oxysterols, while proteins with H/L ratio < 5th percentile in the direct assay and > 95th percentile in the reverse assay were considered down-regulated by oxysterols. Normalized SILAC ratio values, provided by MaxQuant, were used for protein quantification (instead of raw ratio), in order to eliminate experimental bias due to variation in the overall content of heavy and light proteins in each sample.

The list of proteins modulated by the oxysterols was analysed using STRING (version 10) to detect interactions between them and to perform enrichment analysis of gene ontology (GO) categories and KEGG pathways, which were considered “enriched” if the probability of finding the observed number of proteins was < 0.05.

2.8. Immunoblotting

In order to validate the results of SILAC proteomic analysis, an immunoblot was performed. Briefly, HeLa cells or MA104 cells were plated in 6 well plates and treated with 25HC or 27HC at 5 μ M, when they reached confluence. Control samples were prepared by treating cells with culture medium supplemented with equal volumes of ethanol, corresponding to 0.17% (v/v) in cell media. After 20 h, cells were washed twice with sterile PBS, harvested and lysed in denaturing conditions. Extracted proteins were denatured by boiling for 5 min, then separated by 12%-SDS polyacrylamide gel electrophoresis (SDS-12% PAGE) and transferred to a polyvinylidene difluoride (PVDF) membrane. Membranes were blocked overnight at 4 °C with PBS, 0.1%

Tween 20, and milk powder 10%. Membranes were then incubated with the primary antibody for 1 h at 37 °C, washed 4 times with PBS, 0.1% Tween 20, and 15% milk powder, then incubated for 1 h at 37 °C with the secondary antibody coupled with horseradish peroxidase and washed extensively prior to developing by the enhanced chemiluminescence method. The bands’ density was compared using ImageJ software, and the intensity of the actin bands was used to normalize values. Where possible, the results were expressed as a percentage, by comparing treated cells with cells incubated with culture medium alone. Statistically significant differences ($p < 0.05$) were assessed by one-way analysis of variance (one-way ANOVA).

3. Results and discussion

3.1. Detection of proteins modulated by 25HC and 27HC

HeLa cells were challenged 20 h at 37 °C in the presence or in the absence of 25HC or 27HC, at the final concentration of 5 μ M, an oxysterol dose and an incubation time that previously showed to fully abolish Rhinovirus and Rotavirus replication [5]. Notably, the half maximal cytotoxic concentration (CC₅₀) of both oxysterols was shown to be > 150 μ M [5].

In order to obtain a first, large-scale and unbiased view of the effect of the two oxysterols 25HC and 27HC on cells, we applied quantitative proteomics as approach to detect variations of protein expression upon the incubation of model cells with 25HC and/or 27HC.

In particular, stable isotope labelling in cell culture (SILAC) was used as fully established and reliable method to obtain large-scale protein quantification [13]. The HeLa cell line was exploited as model system, not only because largely employed in *in vitro* antiviral studies, including those related to oxysterols [4,5,14–17], but also because successfully applied to several SILAC-based studies [13,18], also in the field of virology [19–21].

According to the SILAC strategy, heavy- and light-labelled cells were treated *in vitro* with 25HC, 27HC or vehicle (sterile-filtered ethanol). After mixing heavy and light cells in 1:1 ratio, proteins were extracted, fractionated, digested, analysed by mass spectrometry, identified, and relatively quantified according to heavy/light SILAC ratios. Overall, more than 3000 proteins were identified in samples obtained from 25HC- and 27HC-treated cells (Table 1).

Rigorous quality filters were applied to focus the analysis on high quality data (as described in the Materials and Methods section). After filtering, the total numbers of proteins genuinely identified and quantified were 2262 and 2,287, in HeLa cells respectively treated with 25HC and 27HC. The overlap between replicate analyses was remarkable: 87.5% of the proteins were identified and quantified in both direct and reverse 25HC assays, and 83.2% of the proteins in the case of the 27HC assays.

Quality filters were applied to focus on genuine identifications and quantifications.

Table 1

Number of proteins identified and quantified in HeLa cells treated with 25HC and 27HC.

	N. of proteins	
	25-HC	27-HC
protein identification (raw)	3081	3135
- reverse database	3043	3105
- contaminants	3008	3068
- id. based on modifications	2965	3025
≥ 2 peptides/protein	2364	2393
≥ 1 unique peptide/protein	2319	2341
≥ 2 SILAC ratio/protein	2262	2287
up-regulated proteins	18	8
down-regulated proteins	38	33

Proteins modulated by 25HC and 27HC were detected by applying 5th and 95th percentile thresholds at the distribution of SILAC ratio obtained in each sample.

Notably, since the main task of the here reported proteomic analysis was to investigate possible mechanisms underlying the antiviral effect displayed in a quite similar way by both oxysterols, we focused on those proteins whose cellular expression was either increased or decreased upon both 25HC and 27HC treatments.

For the sake of completeness, the whole list and details of proteins modulated by each oxysterol are provided in [Supplementary Tables S1–S4](#).

3.2. Proteins up-regulated by both 25HC and 27HC

Table 2 reports the proteins up-regulated in both 25HC- and 27HC-treated HeLa cells, as compared to control cells treated with vehicle.

Among the proteins up-regulated by both oxysterols, only nuclear factor-kappa-B p100 subunit (NFKB2), a transcription factor playing a role in inflammation and immune functions, might actually be related to viral infections but also to the antiviral properties of the two side chain oxysterols. p100 is the precursor protein of NF-kB2/p52; the processing of p100 is signal-dependent and highly inducible, and it selectively degrades the C-terminal portion of the precursor protein, working as an alternative mechanism for NF-kB activation. Indeed, several viruses have been shown to activate NF-kB signalling, usually in the first stages of the infection and in a transient way [22–25]. The NF-kB-dependent induction of inflammatory cytokines synthesis would then contribute to counteract cell invasion by viral particles [26–28] and the recognized pro-inflammatory properties of oxysterols [29,30] could potentiate the cytokine production provoked by the virus, as actually demonstrated in cells infected with Herpes Simplex type 1 virus (HSV-1) [4]. However, even if the proteomic result regarding NF-kB2 well fits with the recent available literature, the same finding should be taken with care due to the high CV observed (**Table 2**).

3.3. Proteins down-regulated by both 25HC and 27HC

Listed in **Table 3** are the proteins down-regulated in both 25HC- and 27HC-treated HeLa cells.

The large majority of the proteins whose cellular content resulted to be significantly reduced by HeLa treatment with 25HC or 27HC is related to lipid synthesis and metabolism or more specifically to sterol synthesis and metabolism. This finding was somehow expected, still the proteome analysis of oxysterol treated cells provided for the first time, to our knowledge, meaningful and precious data. For instance, both investigated oxysterols strongly down-regulated cellular levels of hydroxymethylglutaryl-CoA (HMG-CoA) synthase, the key regulatory enzyme of the cholesterol synthetic pathway. This is consistent with previous literature, showing that 25-HC is a HMG-CoA reductase and synthase inhibitor [31] and, by means of this mechanism, it conveys an antiviral state in treated cells, particularly against flaviviruses, including hepatitis C virus [32]. Moreover, both oxysterols can down-regulate the expression of isopentenyl-diphosphate delta-isomerase 1, a crucial regulatory enzyme in the synthesis of isoprenoids. Interestingly,

an excessive protein isoprenylation is correlated to cardiovascular and age-related disease [33], while the two oxysterols would act as quenchers of isoprenoids' synthesis.

Out of 19 cellular proteins found to be down-regulated by both 25HC and 27HC, three are most likely implicated in viral entry and replication, namely interferon-induced transmembrane protein 3 (IFITM3/Q01628), cation independent mannose-6-phosphate receptor (MPRCi/P11717) and junctional adhesion molecule A (JAM-A/Q9Y624) (**Table 3**).

IFITM3 actually appears to be an antiviral protein inducible by α and γ interferons and acting as restriction factor inhibiting the cell entry of a number of enveloped viruses, such as influenza A virus, Marburg and Ebola filoviruses, SARS coronavirus [34]. IFITM3, like IFITM2, predominantly localizes at the endosomal level and most likely interferes with endocytosis-mediated viral entry and progression in the late endosomes, as observed for IFITM2 in the case of African swine fever virus [35]. Thus, these findings would exclude the IFITM3 falling off induced by 25HC and 27HC as a mechanism underlying their proved antiviral activity.

3.4. Reduced expression of MPRci and JAM-A proteins: two likely antiviral mechanisms of 25HC and 27HC

Contrary to the observed reduction of IFITM3, the down-regulation of MPRci and JAM-A cellular levels as exerted by 25HC and 27HC appears to support the antiviral properties displayed by these side chain oxysterols.

MPRCi, together with the cation dependent isoform MPRcd, is one of the specialized transporters of newly synthesized lysosomal factors, including cathepsins, from the Golgi apparatus to late endosomes (LE) [36]. It was very recently demonstrated that most rotavirus strains need the Golgi-LEs transporters MPRci and Sortilin-1 and their cargo cathepsins to efficiently infect Caco-2 and MA104 cells [37]. In this relation, both 25HC and 27HC proved to markedly inhibit rotavirus replication in the same cell lines [5,6]. In the report of Diaz-Salinas and colleagues [37], at least cathepsins B, L and S were involved in the Golgi-LE traffic modulated by MPRci. SILAC experiments showed a significant down-regulation of cathepsin D only in HeLa cells treated with 25HC and not with 27HC ([Supplementary Material, Table S2](#)). It cannot be excluded that also this isoform could contribute to the infectivity of at least defined rotavirus strains. More importantly, MPR appears to be pivotal for the replication of several other viruses. Vaccinia virus protein p37 localizes to the LE and interacts with proteins associated with LE-derived transport vesicle biogenesis such as MPR to facilitate assembly of extracellular forms of virus [38]. The HSV glycoprotein D (gD), which is essential for this virus to enter cells, can efficiently bind to MPRci, an interaction that plays a role in virus entry and egress [39]. In a recent study, Dohgu and colleagues showed that the MPR is involved in both the replicative cycle and the dissemination of human immunodeficiency virus (HIV-1), facilitating the passing of HIV-1 through the blood brain barrier [40].

It must be outlined the fact that Sortilin-1 was not among the proteins whose cellular level was diminished by the oxysterol treatment, thus a MPRci independent Golgi-LE pathway may compensate the

Table 2
Proteins up-regulated by both 25HC and 27HC

1st ID UniProt	1st Protein name	average ratio 25HC	CV (%) 25HC	average ratio 27HC	CV (%) 27HC
Q00653	Nuclear factor-kappa-B p100 subunit	1.692	31.0	1.399	13.29
Q96QD8	Sodium-coupled neutral amino acid transporter 2	1.731	8.3	1.379	11.22
Q00534	Cyclin-dependent kinase 6	1.280	6.5	1.223	4.89
Q81ZV5	Retinol dehydrogenase10	1.238	6.1	1.212	6.44
O00762	Ubiquitin-conjugating enzyme E2 C	1.310	4.1	1.194	5.19
Q99595	Mitochondrial import inner membrane translocase subunit Tim17-A	1.323	12.3	1.184	2.52

CV: coefficient of variation.

Table 3
Proteins down-regulated by both 25HC and 27HC

1st ID UniProt	1st Protein name	average ratio 25HC	CV (%) 25HC	average ratio 27HC	CV (%) 27HC
P37268	Squalene synthase	0.262	38.5	0.164	26.80
O00767	Acyl-CoA desaturase	0.221	19.3	0.229	1.47
Q01581	Hydroxymethylglutaryl-CoA synthase, cytoplasmic	0.291	45.3	0.287	38.50
Q13907	Isopentenyl-diphosphate Delta-isomerase 1	0.483	11.8	0.457	7.48
Q16850	Lanosterol 14-alpha demethylase	0.619	26.4	0.535	23.53
Q9UBM7	7-Dehydrocholesterol reductase	0.594	5.4	0.592	5.03
Q01628	Interferon-induced trans membrane protein3	0.544	13.0	0.615	11.71
P49327	Fatty acid synthase	0.670	4.8	0.648	4.82
Q9BWD1	Acetyl-CoA acetyltransferase, cytosolic	0.709	7.9	0.691	9.42
P14324	Farnesylpyrophosphate synthase	0.743	6.2	0.711	2.33
Q15738	Sterol-4-alpha-carboxylate 3-dehydrogenase, decarboxylating	0.726	6.1	0.726	1.87
Q9Y624	Junctional adhesion molecule A	0.626	15.3	0.737	16.42
P11717	Cation-independent mannose-6-phosphate receptor	0.658	1.9	0.766	3.23
P05413	Fatty acid-binding protein, heart	0.786	1.1	0.767	9.07
P53396	ATP-citrate synthase	0.798	3.1	0.771	5.14
Q99933	BAG family molecular chaperone regulator 1	0.782	8.7	0.784	7.03
Q15796	Mothers against decapentaplegic homolog (SMAD2)	0.792	2.2	0.796	1.49
P53007	Tricarboxylate transport protein, mitochondrial	0.796	1.6	0.811	3.30
Q96CP2	FLYWCH family member 2	0.799	3.3	0.849	3.82

CV: coefficient of variation.

specific decrease of a given transporter [41]. However, an actual co-involvement of oxysterol-induced deficit of cell MPRci in the protective effect of 25HC and 27HC against rotavirus infection [5,6] could be reinforced by the evidence that defined rotavirus strains, including the human ones, utilize the tight junction protein JAM-A as a co-receptor to enter enterocyte cells [42]. Solid proofs are actually available indicating that several virus families exploit various tight junction proteins to enter, replicate or even exit the target cells, being JAM-A used by reovirus and rotavirus to facilitate the infection process [43].

Of note, JAM-A and MPRci have a different localization in the cell, being the first bounded to the plasma membrane and the second to cytoplasmic membranes. Hence, the tight junction protein appears the first and critical target of viruses, then reaching LE in a second step to enter into the cytosol from those vesicles.

3.5. Confirmation of JAM-A down regulation in HeLa and MA104 cells

The modulation of JAM-A expression by 25HC and 27HC was assessed by immunoblot analysis. The treatment of HeLa cell line with 25HC or 27HC significantly ($p_{ANOVA} < 0.05$) decreased JAM-A protein level by about 40% and 60% respectively (Fig. 1 A, B). The modulation was comparable to the SILAC ratios obtained in the proteomic analysis,

corresponding to 0.626 in the direct assay and 0.737 in the reverse assay. These results were further confirmed by immunoblotting on 25HC- or 27HC-treated MA104 cells (Fig. 1 C, D).

3.6. Modulation of cholesterol and isoprenoid metabolism by 25HC and 27HC

A quite large portion of the proteins that resulted to be either up- or down regulated by one or both the oxysterols of enzymatic origin considered in the present study are involved in the cholesterol or the isoprenoid metabolism. The evidence here provided of a likely modulation of these key cell metabolic pathways by 25HC and/or 27HC is certainly preliminary and in need of deeper investigation by other groups more focused on sterol metabolism. Still, the data reported here should provide some useful clues for such a more focused research.

4. Conclusions

In the present study, we carried out a technically advanced proteomic screening in a cell model system (HeLa cell line) commonly employed to in vitro test the antiviral efficacy of a wide variety of compounds. Cellular treatment was performed at a concentration of the

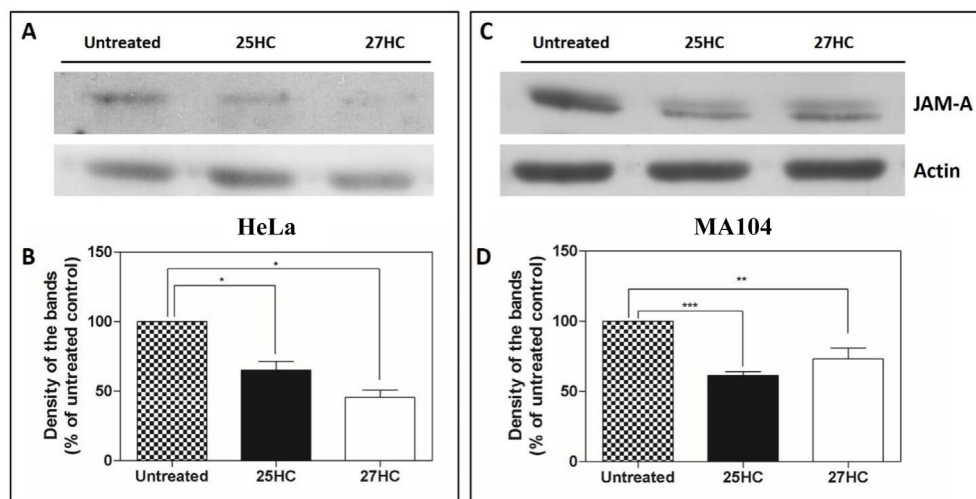


Fig. 1. Western blotting validation of the 25HC- and 27HC-exerted down-regulation of JAM-A protein level in two different cell lines. Cells were incubated 20 h at 37 °C in the presence or in the absence of 25HC or 27HC at 5 μM final concentration. Panels A–C: JAM-A immunoblots were assessed in HeLa and MA104 cells respectively and normalized against actin. Panel B–D: the density of the bands obtained in HeLa and MA104 cells was calculated by means of ImageJ software, using the intensity of the actin bands for values normalization. Results were expressed as percent values as to untreated cells, taken as control. Error bars represent the standard error of the mean (SEM) of two independent experiments in duplicate. Statistically significant differences were assessed by one way analysis of variance (one way ANOVA). * $p_{ANOVA} < 0.05$; ** $p_{ANOVA} < 0.01$; *** $p_{ANOVA} < 0.001$.

two oxysterols (5 μ M) demonstrated to significantly inhibit viral replication of a large number of viral pathogens, without inducing any cytotoxicity at all [1,4–6].

Focusing on the antiviral activity of the two oxysterols, we identified two new mechanisms of inhibition of virus entry and diffusion within infected cells. Indeed, both 25HC and 27HC were shown able to down-regulate the junction adhesion molecule-A and the cation independent isoform of mannose-6-phosphate receptor, two crucial molecules for a number of viruses to exert infection.

This research communication is the first report on cell proteome modulation by two side chain oxysterols, i.e. 25HC and 27HC, certainly of primary interest in human pathophysiology. The two oxysterols were shown by our group to further up-regulate the redox sensitive transcription factor NF- κ B in virus infected cells, by this way boosting the cellular pro-inflammatory reaction against the virus itself [4]. In addition, we previously reported that the survival signalling triggered by low micromolar concentrations of 27HC in the human pro-monocytic U-937 cell line was dependent on a rapid and transient activation of NADPH-oxidase with consequent H₂O₂ production [44,45]. These findings are thus indicating a promising way to deeper elucidate the actual contribution of redox reactions in the antiviral effects of 25HC and 27HC.

Acknowledgements

This study was supported in part by a grant from the University of Torino, Italy (RILO17).

Appendix A. Supplementary data

Supplementary data to this article can be found online at <https://doi.org/10.1016/j.freeradbiomed.2019.08.031>.

References

- [1] S.-L. Liu, R. Aliyari, K. Chikere, G. Li, M.D. Marsden, J.K. Smith, O. Pernet, H. Guo, R. Nusbaum, J.A. Zack, A.N. Freiberg, L. Su, B. Lee, G. Cheng, Interferon-inducible cholesterol-25-hydroxylase broadly inhibit viral entry by production of 25-hydroxycholesterol, *Immunity* 38 (2013) 92–105.
- [2] M. Blanc, W.Y. Hsieh, K.A. Robertson, K.A. Kropp, T. Forster, G. Shui, P. Lacaze, S. Watterson, S.J. Griffiths, N.J. Spann, A. Meljon, S. Talbot, K. Krishnan, D.F. Covey, M.R. Wenk, M. Craigmiles, Z. Ruzsics, J. Haas, A. Angulo, W.J. Griffiths, C.K. Glass, Y. Wang, P. Gazhal, The transcription factor STAT-1 couples macrophage synthesis of 25-hydroxycholesterol to the interferon antiviral response, *Immunity* 38 (2013) 106–118.
- [3] D. Lembo, V. Cagno, A. Civra, G. Poli, Oxysterols: an emerging class of broad spectrum antiviral effectors, *Mol. Syst. Med.* 49 (2016) 23–30.
- [4] V. Cagno, A. Civra, D. Rossin, S. Calafapietra, C. Caccia, V. Leoni, N. Dorma, F. Biasi, G. Poli, D. Lembo, Inhibition of herpes simplex-1 virus replication by 25-hydroxycholesterol and 27-hydroxycholesterol, *Redox Biol.* 12 (2017) 522–527.
- [5] A. Civra, V. Cagno, M. Donalisio, F. Biasi, G. Leonarduzzi, G. Poli, D. Lembo, Inhibition of pathogenic non-enveloped viruses by 25-hydroxycholesterol and 27-hydroxycholesterol, *Sci. Rep.* 4 (2014) 7487, <https://doi.org/10.1038/srep07487>.
- [6] A. Civra, R. Francese, P. Gamba, G. Testa, V. Cagno, G. Poli, D. Lembo, 25-Hydroxycholesterol and 27-hydroxycholesterol inhibit human rotavirus infection by sequestering viral particles into late endosomes, *Redox Biol.* 19 (2018) 318–330.
- [7] X. Li, P. Hylemon, W.M. Pandak, S. Ren, Enzyme activity assay for cholesterol 27-hydroxylase in mitochondria, *J. Lipid Res.* 47 (2006) 1507–1512.
- [8] V. Leoni, C. Caccia, Potential diagnostic applications of side chain oxysterols analysis in plasma and cerebrospinal fluid, *Biochem. Pharmacol.* 86 (2013) 26–36.
- [9] L.J. Ward, S.A. Liunggren, H. Karlsson, W. Li, X.M. Yuan, Exposure to atheroma-relevant 7-oxysterols causes proteomic alterations in cell death, cellular longevity, and lipid metabolism in THP-1 macrophages, *PLoS One* 12 (2017) e0174475, <https://doi.org/10.1371/journal.pone.0174475>.
- [10] L. Rosa-Fernandes, L.M.F. Maselli, N.Y. Maeda, G. Palmisano, S.P. Bydlowski, Outside-in, inside-out: proteomic analysis of endothelial stress mediated by 7-ke-tocholesterol, *Chem. Phys. Lipids* 207 (Pt B) (2017) 231–238.
- [11] F. Schmidt, M. Strozynski, S.S. Salus, H. Nilsen, B. Thiede, Rapid determination of amino acid incorporation by stable isotope labelling with amino acids in cell culture (SILAC), *Rapid Commun. Mass Spectrom.* 21 (2007) 3919–3926.
- [12] J. Cox, M. Mann, MaxQuant enables high peptide identification rates, individualized p.p.b.-range mass accuracies and proteome-wide protein quantification, *Nat. Biotechnol.* 26 (2008) 1367–1372.
- [13] S.E. Ong, M. Mann, A practical recipe for stable isotope labeling by amino acids in cell culture (SILAC), *Nat. Protoc.* 1 (2006) 2650–2660.
- [14] P.S. Roulin, M. Lötzerich, F. Torta, L.B. Tanner, F.J. van Kuppeveld, M.R. Wenk, U.F. Greber, Rhinovirus uses a phosphatidylinositol 4-phosphate/cholesterol counter-current for the formation of replication compartments at the ER-Golgi interface, *Cell Host Microbe* 16 (2014) 677–690.
- [15] P.S. Roulin, L.P. Murer, U.F. Greber, A single point mutation in the Rhinovirus 2B protein reduces the requirement for phosphatidylinositol 4-kinase class III beta in viral replication, *J. Virol.* 92 (2018), <https://doi.org/10.1128/JVI.01462-18.e01462-18>.
- [16] A. Doms, T. Sanabria, J.N. Hansen, N. Altan-Bonnet, G.H. Holm, 25-Hydroxycholesterol production by the cholesterol-25-hydroxylase Interferon-stimulated gene restricts mammalian Reovirus infection, *J. Virol.* 92 (2018), <https://doi.org/10.1128/JVI.01047-18.e01047-18>.
- [17] H. Wang, J.W. Perry, A.S. Lauring, P. Neddermann, R. De Francesco, A.W. Tai, Oxysterol-binding protein is a phosphatidylinositol 4-kinase effector required for HCV replication membrane integrity and cholesterol trafficking, *Gastroenterology* 146 (2014) 1373–1385.
- [18] M. Hilger, M. Mann, Triple SILAC to determine stimulus specific interactions in the Wnt pathway, *J. Proteome Res.* 11 (2012) 982–994.
- [19] K.M. Coombs, HeLa cell response proteome alterations induced by mammalian reovirus T3D infection, *Virol. J.* 10 (2013) 202, <https://doi.org/10.1186/1743-422X-10-202>.
- [20] L.K. Zhang, F. Chai, H.Y. Li, G. Xiao, L. Guo, Identification of host proteins involved in Japanese encephalitis virus infection by quantitative proteomics analysis, *J. Proteome Res.* 12 (2013) 2666–2678.
- [21] Y.W. Lam, V.C. Evans, K.J. Heesom, A.I. Lamond, D.A. Matthews, Proteomics analysis of the nucleolus in adenovirus-infected cells, *Mol. Cell. Proteom.* 9 (2010) 117–130.
- [22] L. Havard, S. Rahmouni, J. Boniver, P. Delvenne, High levels of p105 (NFKB1) and p100 (NFKB2) proteins in HPV16-transformed keratinocytes: role of E6 and E7 oncoproteins, *Virology* 331 (2005) 357–366.
- [23] I. Erising, K. Bernhardt, B.E. Gewurz, NF- κ B and IRF7 pathway activation by Epstein-Barr virus latent membrane protein 1, *Viruses* 5 (2013) 1587–1606.
- [24] G. Jiang, S. Dandekar, Targeting NF- κ B signaling with protein kinase C agonists as an emerging strategy for combating HIV latency, *AIDS Res. Hum. Retrovir.* 31 (2015) 4–12.
- [25] R.M.G. Da Costa, M.M.S.M. Bastos, R. Medeiros, P.A. Oliveira, The NF κ B signaling pathway in papillomavirus-induced lesions: friend or foe? *Anticancer Res.* 36 (2016) 2073–2083.
- [26] T.H. Mogensen, J. Melchjorsen, L. Malmgaard, A. Casola, S.R. Paludan, Suppression of proinflammatory cytokine expression by herpes simplex virus type 1, *J. Virol.* 78 (2004) 5883–5890.
- [27] A.J. Chucair-Elliott, C. Conrady, M. Zheng, C.M. Kroll, T.E. Lane, D.J. Carr, Microglia-induced IL-6 protects against neuronal loss following HSV-1 infection of neural progenitor cells, *Glia* 62 (2014) 1418–1434.
- [28] E.A. Murphy, J.M. Davis, A.S. Brown, M.D. Carmichael, A. Ghaffar, E.P. Mayer, Effect of IL-6 deficiency on susceptibility to HSV-1 respiratory infection and intrinsic macrophage antiviral resistance, *J. Interferon Cytokine Res.* 28 (2008) 589–595.
- [29] G. Leonarduzzi, P. Gamba, S. Gargiulo, F. Biasi, G. Poli, Inflammation-related gene expression by lipid oxidation-derived products in the progression of atherosclerosis, *Free Radic. Biol. Med.* 52 (2012) 19–34.
- [30] S. Gargiulo, G. Testa, P. Gamba, E. Staurenghi, G. Poli, G. Leonarduzzi, Oxysterols and 4-hydroxy-2-nonenal contribute to atherosclerotic plaque destabilization, *Free Radic. Biol. Med.* 111 (2017) 140–150.
- [31] J.P. Pezacki, S.M. Sagan, A.M. Tonary, Y. Rouleau, S. Bélanger, L. Supekova, A.I. Su, Transcriptional profiling of the effects of 25-hydroxycholesterol on human hepatocyte metabolism and the antiviral state it conveys against the hepatitis C virus, *BMC Chem. Biol.* 9 (2009), <https://doi.org/10.1186/1472-6769-9-2>.
- [32] J.F. Osuna-Ramos, J.M. Reyes-Ruiz, R.M. Del Ángel, The role of host cholesterol during Flavivirus infection, *Front. Cell. Infect. Microbiol.* 8 (2018), <https://doi.org/10.3389/fcimb.2018.00388>.
- [33] D. Perez-Sala, Protein isoprenylation in biology and disease: general overview and perspectives from studies with genetically engineered animals, *Front. Biosci.* 12 (2007) 4456–4472.
- [34] I.C. Huang, C.C. Bayley, J.L. Weyer, S.R. Radoshitzky, M.M. Becker, A.L. Brass, A.A. Ahmed, X. Chi, L. Dong, L.E. Longobardi, D. Boltz, J.H. Kuhn, S.J. Elledge, S. Bavari, M.R. Denison, H. Choe, M. Farzan, Distinct patterns of IFITM-mediated restriction of filoviruses, SARS coronavirus, and influenza A virus, *PLoS Pathog.* 7 (2011) e1001258, <https://doi.org/10.1371/journal.ppat.1001258>.
- [35] R. Muñoz-Moreno, M.A. Cuesta-Geijo, C. Martínez-Romero, L. Barrado-Gil, I. Galindo, A. García-Sastre, A. Covadonga, Antiviral role of IFITM proteins in African Swine Fever virus infection, *PLoS One* 11 (2016) e0154366, <https://doi.org/10.1371/journal.pone.0154366>.
- [36] T. Braulke, J.S. Bonifacino, Sorting of lysosomal proteins, *Biochim. Biophys. Acta* 1793 (2009) 605–614.
- [37] M.A. Díaz-Salinas, L.A. Casorla, T. López, S. López, C.F. Arias, Most rotavirus strains require the cation-independent mannose-6-phosphate receptor, sortilin-1, and cathepsins to enter cells, *Virus Res.* 245 (2018) 44–51.
- [38] Y. Chen, K.M. Honeychurch, G. Yang, C.M. Byrd, C. Harver, D.E. Hruby, R. Jordan, Vaccinia virus p37 interacts with host proteins associated with LE-derived transport vesicle biogenesis, *Virol. J.* 6 (2009) 44, <https://doi.org/10.1186/1472-6769-9-2>.
- [39] M. Gary-Bobo, P. Nirdé, A. Jeanjean, A. Morère, M. Garcia, Mannose 6-phosphate receptor targeting and its applications in human diseases, *Curr. Med. Chem.* 14 (2007) 2945–2953.
- [40] S. Dohgu, J.S. Ryerse, S.M. Robinson, W.A. Banks, Human immunodeficiency virus-1 uses the mannose-6-phosphate receptor to cross the blood-brain barrier, *PLoS One*

- 7 (2012) e39565, , <https://doi.org/10.1371/journal.pone.0039565>.
- [41] M.F. Coutinho, M.J. Prata, S. Alves, A shortcut to the lysosome: the mannose-6-phosphate-independent pathway, *Mol. Genet. Metab.* 107 (2012) 257–266.
- [42] J.M. Torres-Flores, D. Silva-Ayala, M.A. Espinoza, S. López, C.F. Arias, The tight junction protein JAM-A functions as coreceptor for rotavirus entry into MA104 cells, *Virology* 475 (2015) 172–178.
- [43] J.M. Torres-Flores, C.F. Arias, Tight junctions go viral!, *Viruses* 7 (2015) 5145–5154.
- [44] B. Vurusaner, P. Gamba, G. Testa, S. Gargiulo, F. Biasi, C. Zerbinati, L. Iuliano, G. Leonarduzzi, H. Basaga, G. Poli, Survival signaling elicited by 27-hydroxycholesterol through the combined modulation of cellular redox state and ERK/Akt phosphorylation, *Free Radic. Biol. Med.* 77 (2014) 376–385.
- [45] B. Vurusaner, G. Leonarduzzi, P. Gamba, G. Poli, H. Basaga, *Mol. Asp. Med.* 49 (2016) 8–22.